Accepted Manuscript

Continued SAR exploration of 1,2,4-thiadiazole-containing scaffolds in the design of free fatty acid receptor 1 (GPR40) agonists

Mikhail Krasavin, Alexei Lukin, Anna Bakholdina, Nikolay Zhurilo, Oleksandra Onopchenko, Petro Borysko, Sergey Zozulya, Daniel Moore, Irina G. Tikhonova

PII: S0223-5234(17)30701-8

DOI: 10.1016/j.ejmech.2017.09.019

Reference: EJMECH 9734

To appear in: *European Journal of Medicinal Chemistry*

Received Date: 14 July 2017

Revised Date: 10 September 2017

Accepted Date: 11 September 2017

Please cite this article as: M. Krasavin, A. Lukin, A. Bakholdina, N. Zhurilo, O. Onopchenko, P. Borysko, S. Zozulya, D. Moore, I.G. Tikhonova, Continued SAR exploration of 1,2,4-thiadiazole-containing scaffolds in the design of free fatty acid receptor 1 (GPR40) agonists, *European Journal of Medicinal Chemistry* (2017), doi: 10.1016/j.ejmech.2017.09.019.

Continued SAR Exploration of 1,2,4-Thiadiazole-containing Scaffolds in the Design of Free Fatty Acid Receptor 1 (GPR40) agonists

Mikhail Krasavin, Alexei Lukin, Anna Bakholdina, Nikolay Zhurilo, Oleksandra Onopchenko, Petro Borysko, Sergey Zozulya, Daniel Moore, and Irina G. Tikhonova

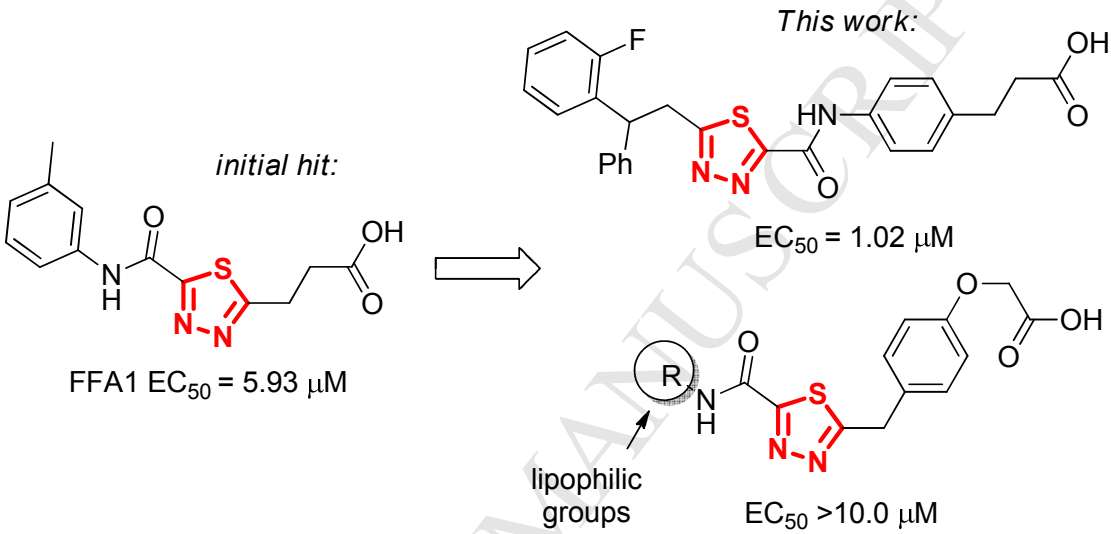

Continued SAR Exploration of 1,2,4-Thiadiazole-containing Scaffolds in the Design of Free Fatty Acid Receptor 1 (GPR40) agonists

Mikhail Krasavin[1,*], Alexei Lukin[2], Anna Bakholdina[2], Nikolay Zhurilo[2], Oleksandra Onopchenko[3], Petro Borysko,[3] Sergey Zozulya[3,4], Daniel Moore[5], and Irina G. Tikhonova[5]

[1] Saint Petersburg State University, Saint Petersburg, 199034 Russian Federation

[2] Lomonosov Institute of Fine Chemical Technologies, Moscow Technological University, Moscow, 117571 Russian Federation

[3] Enamine Ltd, Kyiv 02094, Ukraine

[4] Taras Shevchenko National University, 62 Volodymyrska, Kyiv 01033, Ukraine

[5] Molecular Therapeutics, School of Pharmacy, Medical Biology Centre, Queen's University Belfast, Northern Ireland, UK

* Corresponding author: Mikhail Krasavin, Institute of Chemistry, Saint Petersburg State University, 26 Universitetskyi prospect, Peterhof 198504 Russia. E-mail: m.krasavin@spbu.ru Fax: +7 812 428 6939.

An earlier reported series of 1,2,4-thiadiazole-based agonists of FFA1 (GPR40) was evolved into two structurally distinct series of compounds. One of the series (structurally related to known FFA1 agonist GW9508) displayed low micromolar potency while the other (representing a truncated version of the earlier reported potent FFA1 agonists) was, surprisingly, found to be devoid of agonist potency. *In silico* docking of representative compounds into the crystal structure of FFA1 revealed possible structural grounds for the observed SAR.

Keywords: free fatty acid receptor 1; GPR40; 1,2,4-thiadiazole; heterocyclic bioisosteres; agonist potency; *in silico* docking.

1. Introduction

The deorphanization of GPR40 as free fatty acid receptor 1 (FFA1) in 2003 and the demonstration of its involvement in the regulation of insulin secretion [1] offered much hope for the development of novel therapeutic approach to the treatment of type II diabetes mellitus. This resulted in an intense drug discovery race that have led to numerous advanced agonists among which compounds incorporating 3-phenylpropanoic acid moiety (such as TAK-875, AMG 837, GW9508 and LY2881845 shown in Fig. 1) are notable [2]. Unfortunately, this area of drug development was adversely affected by the discontinuation of TAK-875 (fasiglifam) in the course of phase III clinical trials, when the hepatotoxicity risk outweighed the benefit of reducing the blood glucose levels in patients [3]. The latter aspect, despite the fate of fasiglifam, constitutes a proof of concept [4] for the new therapeutic approach involving activation of FFA1 in pancreatic β-cells. Therefore, development of new FFA1 agonists devoid of toxic effects in the liver can revive this class of potentially life-saving antidiabetic therapies [5]. Hepatotoxicity of fasiglifam may be caused by the lipophilic character of its 3-phenylpropanoic acid core [6-8] and, therefore, various heterocyclic replacements of the phenyl ring in this important FFA1 pharmacophore [9-12] as well as introduction of peripheral polar motifs [13-15] represent a viable drug design strategy.

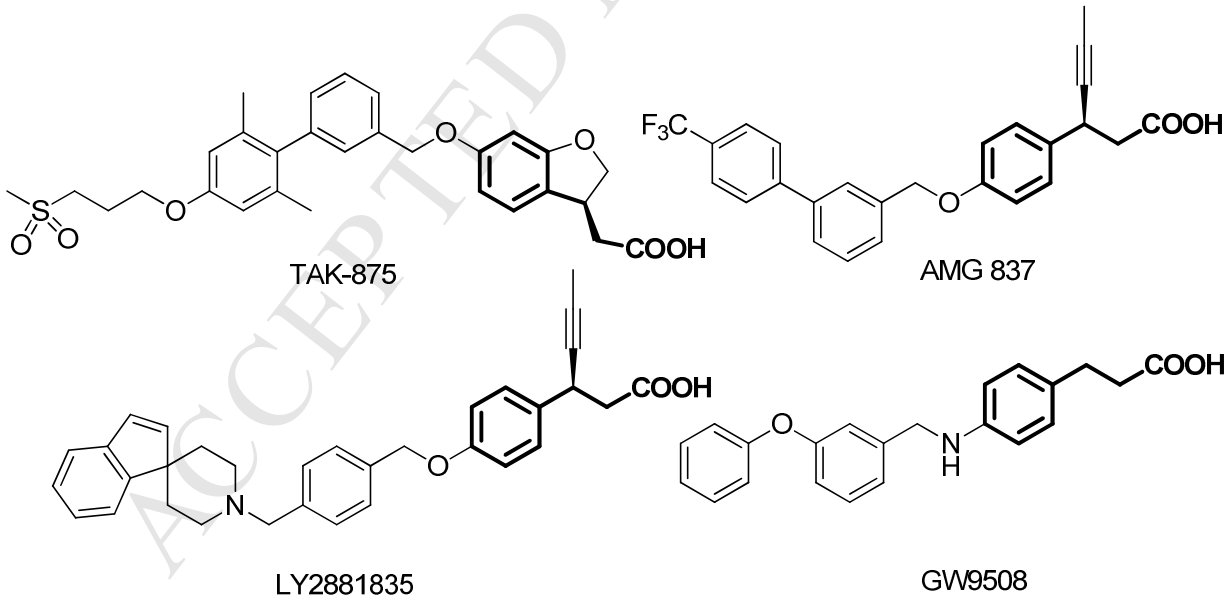

Fig. 1. GPR40 agonists based on 3-phenylpropanoic acid core.

Last year, we reported 1,2,4-thiadiazole **1** as a moderately potent FFA1 agonist [16]. Its subsequent medicinal chemistry evolution led to more potent compounds **2** and **3** [17]. More recently, we have continued the exploration of 1,2,4-thiadiazole core as a basis for FFA1 agonist

design. Herein, we report the synthesis and biological evaluation, for FFA1 activation, of two novel 1,2,4-thiadiazole-based compound series – **4** and **5** (Fig. 2).

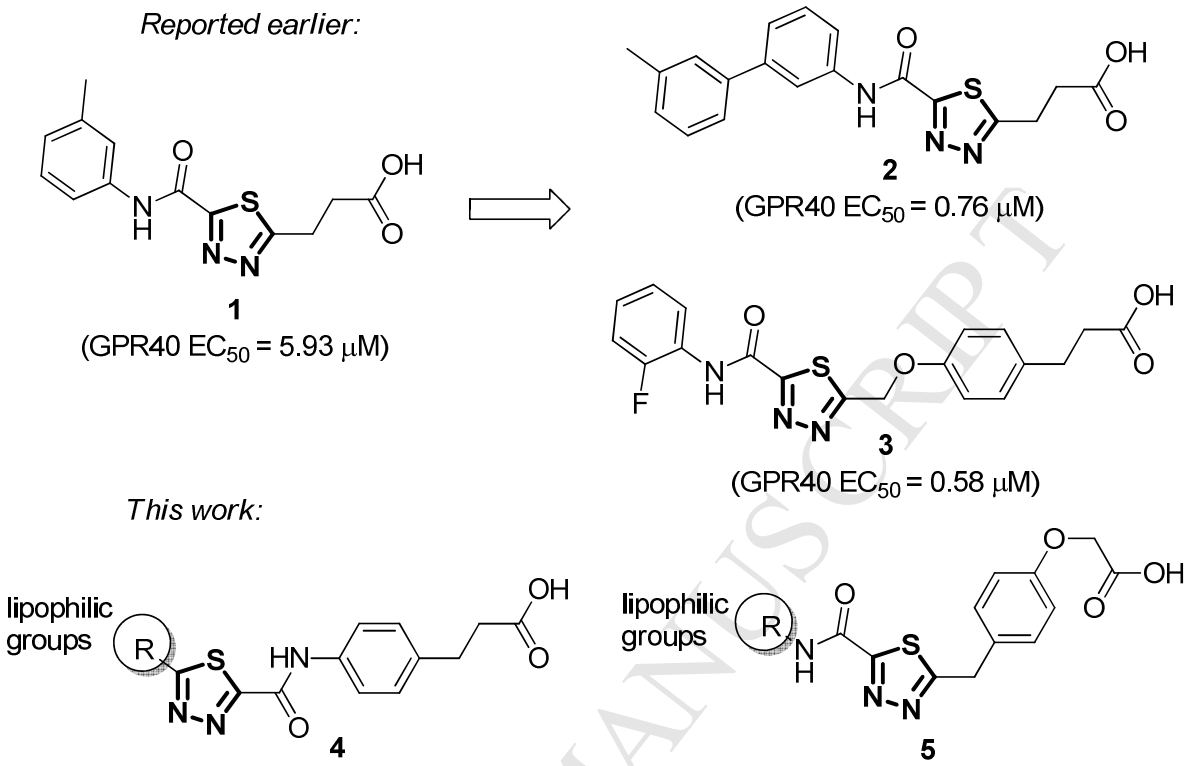

Fig. 2. 1,2,4-Thiadiazole-based FFA1 agonists reported by us earlier (**1**-**3**) [16-17] and explored in this work (**4**-**5**).

The former series can be viewed as congeners of GW9508 where 3-(phenoxy)benzyl portion is replaced by 1,3,4-thiadiazole-2-carbonyl moiety bearing lipophilic periphery groups. Series **5** is closely related to compound **3**, in which the oxygen atom was removed from the linker between the 1,2,4-thiadiazole and phenyl moieties (thus shortening it) and replaced one of the methylene groups in the 3-phenylpropionic acid moiety (representing a recently reported viable FFA1 agonist modification [18]).

2. Results and discussion

2.1 Chemistry

The two series investigated in this work – **4** and **5** - were accessed via a similar strategy involving acylation of the thiosemicarbazide terminal nitrogen followed by cyclodehydration in glacial acetic acid [16]. For the preparation of compounds **4a-t**, known *tert*-butyl ester **6** [19] was acylated with chloroacetyl chloride. The resulting derivative, without isolation, was transformed into thiosemicarbazide **7** via the treatment with elemental sulfur, triethylamine and morpholine (triggering a Willgerodt-Kindler-type reaction) followed by the addition of hydriazine hydrate.

Acylation of **7** with a series of commercially available carboxylic acids **8a-t** activated by carbonyl-1,1′-diimidazole (CDI) followed by cyclodehydration in refluxing glacial acetic acid and removal of *tert*-butyl group gave compounds **4a-t** in fair to excellent yields (*vide infra*). Similarly, known carboxylic acid **9** [20] activated by CDI was employed in the acylation of a series of thiosemicarbazides **10a-q** (prepared as described previously [16]). The resulting adducts, without isolation, were subjected to the cyclodehydration/*tert*-butyl ester hydrolysis routine to deliver compounds **5a-q** (Scheme 1).

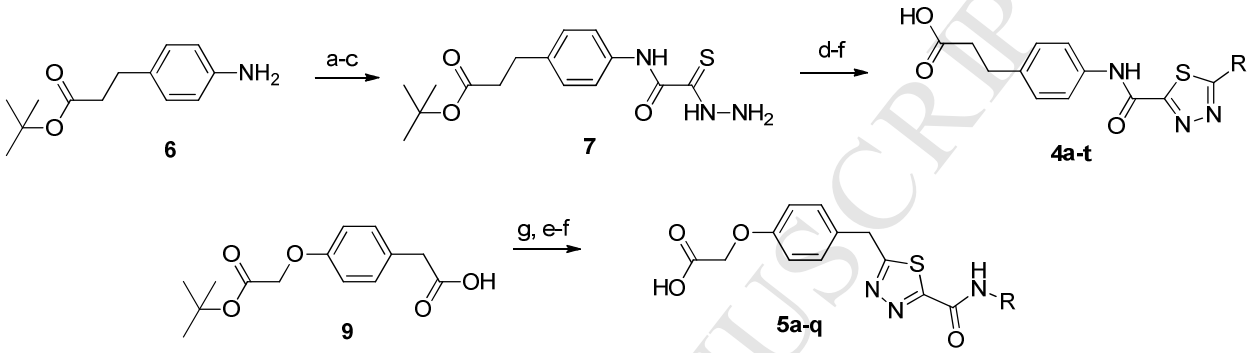

Scheme 1. Preparation of compounds **4a-t** and **5a-q**.

Reagents and conditions: (a) chloroacetyl chloride, Et_3N, THF, 0 ºC → r. t.; (b) S, morpholine, Et_3N, DMF, r. t., 16 h; (c) $N_2H_4 \cdot H_2O$, DMF, r. t., 16 h; (d) RCOOH (**8a-t**), CDI, DCM, r. t., 16 h; (e) glacial AcOH, reflux, 30 min; (f) 4M HCl in 1,4-dioxane, r. t., 16 h; (g) $ArNHCOC(S)NHNH_2$ (**10a-q**).

2.2 Biological activity

All compounds synthesized as described above were tested for FFA1 activation using calcium flux assay employing Chinese hamster ovary (CHO) cells engineered to stably express human FFA1. All compounds were first tested in a single-concentration (% FFA1 activation at 10 μM) format using 10 μM concentration of full agonist GW9508 [21] as a positive control. Compounds which displayed >30% FFA1 activation were tested in dose-response mode (see Experimental) in order to determine their EC_{50} values.

As can be seen from Table 1, all compounds **4** displayed substantial FFA1 activation in single-concentration experiments and their EC_{50} values were determined to be in the low-micromolar range. The FFA1 affinity of compounds **4a-t** appears to be relatively insensitive to steric or electronic effects in the variable lipophilic portion of the molecule. However, addition of a second aromatic group in compounds **4m-p** noticeably enhanced the potency, which can be attributed to the lipophilicity contribution to the FFA1 affinity [22]. This strongly supports the

fundamental correctness of the series design, i. e. the possibility to replace the lipophilic periphery of GW9508 with 1,2,4-thiazole-3-carboxamide moiety (rich in hydrogen-bond donors and acceptors) bearing lipophilic groups. This view is further supported by the findings from the *in silico* modeling experiments (*vide infra*).

At the same time, all compounds **5a-q** were found to be devoid of any agonism with respect to FFA1. This discovery sets substantial SAR boundaries to the variation of the substituents around the 3-phenylpropanoic acid pharmacophore or, in this case, its phenoxyacetic acid isostere. Indeed, Compounds **5a-q** can be viewed as minimally truncated isosteres of compounds **3** which delivered compounds of submicromolar potency [15]. Apparently, positioning of the 1,2,4-thiazole-3-carboxamide moiety one atom closer to the carboxylic acid terminus completely ablates the antagonist potency.

Table 1. Activation of FFA1 by compounds **4a-t** and **5a-q**.

Compound	R	% FFA1 activation (1 μM)[a]	EC_{50}, μM [b]
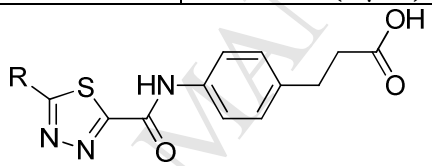			
4a	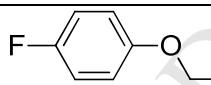	48.5	5.39
4b		88.2	1.53
4c	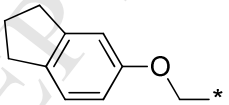	91.2	1.38
4d	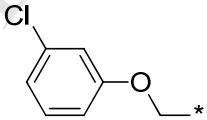	82.9	1.57
4e	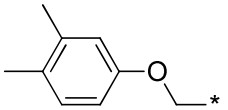	64.9	1.13
4f	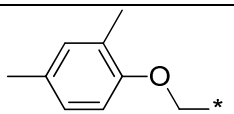	74.7	2.54
4g	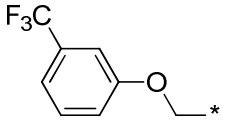	70.1	3.09

4h	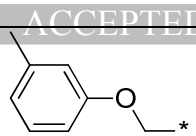	82.4	3.26
4i	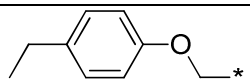	74.4	1.17
4j	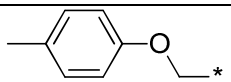	76.9	2.17
4k	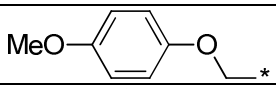	72.5	2.43
4l	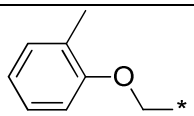	89.9	1.52
4m	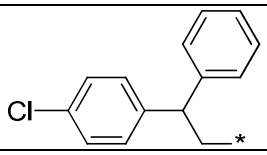	84.9	2.71
4n	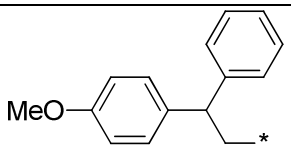	78.9	1.35
4o	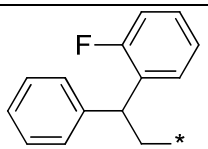	68.6	1.02
4p	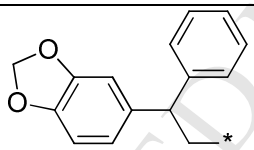	60.3	4.12
4q	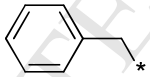	70.1	3.67
4r	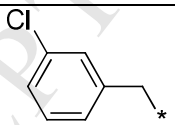	79.4	2.39
4s	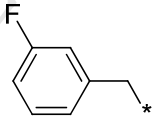	60.3	5.02
4t	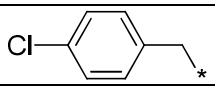	72.3	2.39
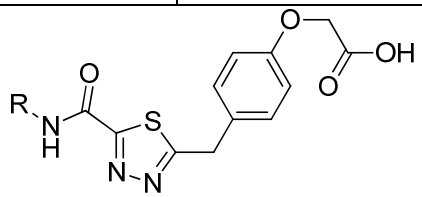			
5a	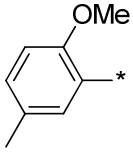	6.6	>10.0

5b	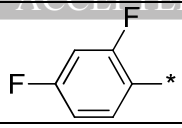	6.6	>10.0
5c	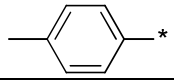	7.0	>10.0
5d	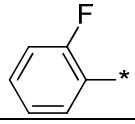	6.0	>10.0
5e	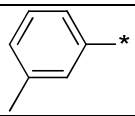	6.0	>10.0
5f	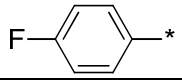	6.0	>10.0
5g	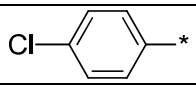	4.2	>10.0
5h	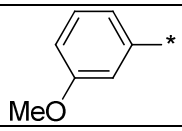	9.2	>10.0
5i	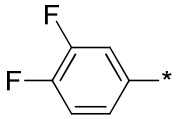	6.6	>10.0
5j	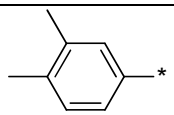	2.8	>10.0
5k	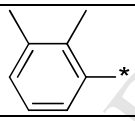	6.6	>10.0
5l	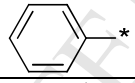	7.8	>10.0
5m	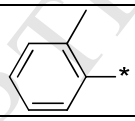	6.6	>10.0
5n	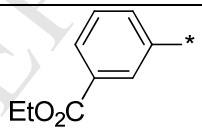	6.4	>10.0
5o	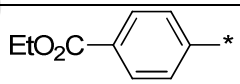	9.4	>10.0
5p	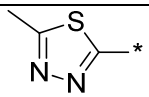	9.8	>10.0
5q	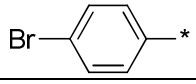	5.9	>10.0

[a] Determined relative to the activation of FFA1 by 10 μM concentration of GW9508.

[b] Each value is an average of n = 4 in the presence of 0.5% DMSO (see Supporting Information).

All active FFA1 agonists (**4a-t**) were not found to display any appreciable agonistic activity when tested at 10 μM concentration (in quadruplicates) against CHO cell lines stably overexpressing other free fatty acid receptors (FFA3/GPR41, FFA2/GPR43 and FFA4/GPR120).

2.3 In silico modeling

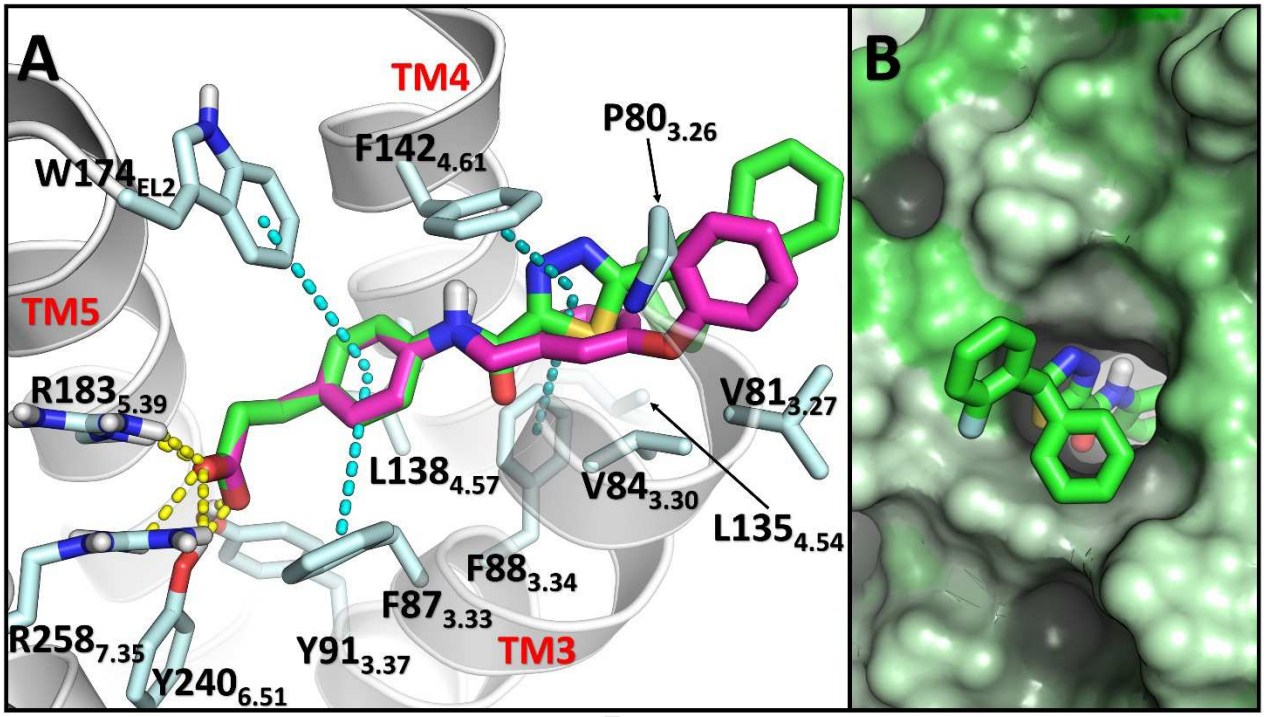

Fig. 3. Docked poses of GW9508 and **4o** at FFA1. (A) Overlay of GW9508 and **4o** in the FFA1 binding site. GW9508 and **4o** are in green and magenta color, respectively. Protein–ligand interactions are visualized for **4o** only. (B) Surface representation of FFA1 with the terminal bis-aromatic tail of **4o**. Hydrogen bonds and π–π interactions are in a yellow and blue dashed-line, respectively. The FFA1 surface is coloured according to the normalized consensus hydrophobicity scale [23] ranging from green to white (less to more hydrophobic). Residues are labeled with their position followed by the Ballesteros and Weinstein numbering [24] Transmembrane helices are labeled in red.

To rationalize the observed submicromolar potency of compound **4o** we docked this compound and the potent agonist GW9508 into the FFA1 binding site, Fig. 3A. The phenylpropanoic acid moiety of the docked compounds adopts an identical position within the binding cavity forming the critical hydrogen bonds with $Y91_{3.37}$, $R183_{5.39}$, $Y240_{6.51}$ and $R258_{7.35}$. This inner core is further stabilized by a complex network of π–π interactions occurring between $F88_{3.34}$, $F87_{3.33}$, $F142_{4.61}$ and $W174_{EL2}$ of the receptor and the aromatic rings of the ligands. The hydrophilic 1,2,4-thiadizole is well accommodated in the gap between the transmembrane (TM) helices 3 and 4 adopting a similar conformation as the equivalent benzene ring of GW9508. The role of the 2-(4-fluorophenyl)-2-(phenyl)ethyl tail of **4o** is to lock the inner moiety into a stable position, which is achieved by burying the aromatic tail of the compound within the hydrophobic pocket

of $P80_{3.26}$, $V81_{3.27}$, $V84_{3.30}$ and $L135_{4.54}$ located at the interface with the phospholipid tails of the bi-layer, Figure 3B. It appears that the more hydrophobic extension added to the 1,2,4-thiadizole likely attributes to the ligand ability to bury within this hydrophobic pocket and hence results in better stabilization of the complex leading to the improved potency.

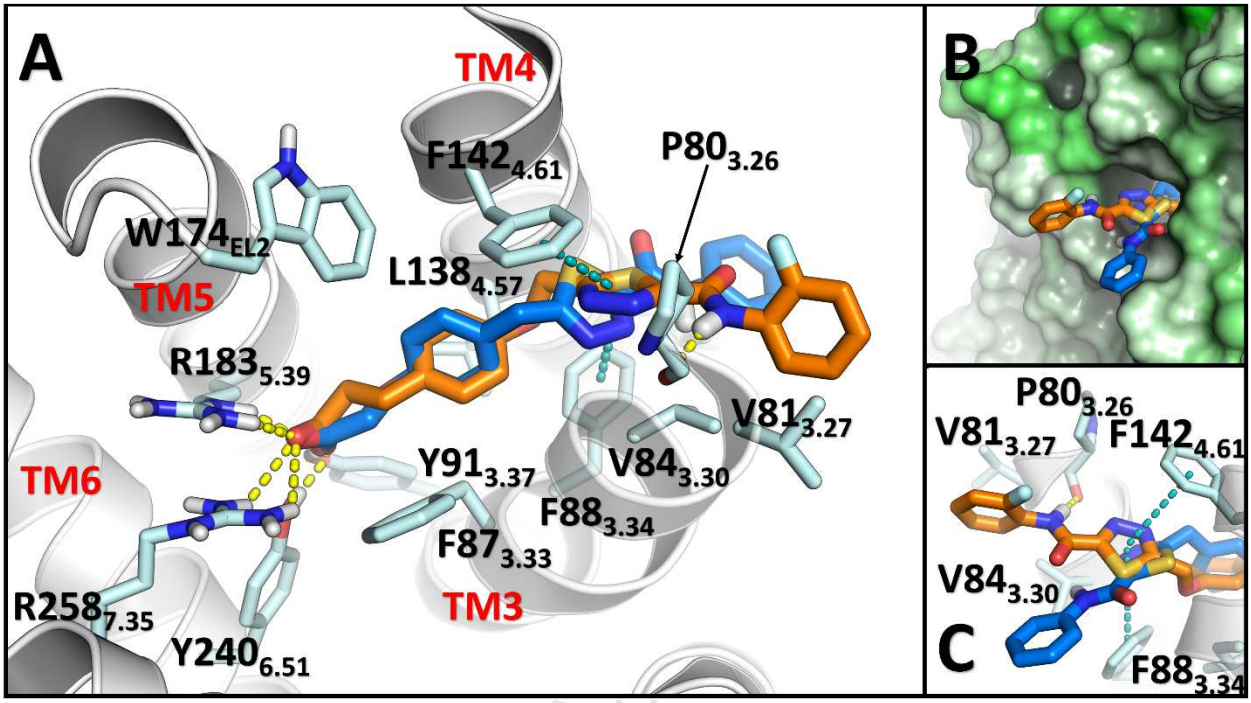

Figure 4. Docked poses of **5l** and **3** at FFA1. (A) Overlay of **5l** and **3** in the FFA1 binding site. **5l** and **3** are in blue and orange color, respectively. Protein–ligand interactions are visualized for compound **3** only. (B) Surface representation of FFA1 with an overlay of the terminal tails of **5l** and **3**. (C) Overlay of the terminal moieties of **5l** and **3** visualizing the interactions occurring between the terminal moiety and TM3 and TM4 of FFA1. Hydrogen bonds and π–π interactions are in a yellow and blue dashed-line, respectively. Surface is coloured according to the normalized consensus hydrophobicity scale [20] ranging from green to white (less to more hydrophobic). Residues are labeled with their position followed by the Ballesteros and Weinstein numbering [21]. Transmembrane helices are labeled in red.

In order to understand the structural alterations that resulted in the loss of potency observed with series **5**, we docked compound **5l** and compound **3** from our previous study [26], which differs by having an additional atom linker between the phenylpropanoic acid head and the 1,2,4-thiadizole. As visualized in Fig. 4A, despite the structural similarity, the conformations of both compounds are significantly different. Here, the loss of the additional atom linker forces **5l** into an unfavorable position between TM3 and TM4 whereby the steric hindrance between the helices and 1,2,4-thiadizole forces the tail of **5l** to point straight out of the binding cavity (Fig. 4B), which leads to the loss of the critical hydrogen bond with the backbone of $P80_{3.26}$. Furthermore, this prevents the tail from burying within the hydrophobic pocket of TM3 consisting of $P80_{3.26}$, $V81_{3.27}$ and $V84_{3.30,}$ which otherwise facilitates the binding of the ligand

(Fig. 4C). Indeed, a flexible extension onto the phenoxyacetic acid core would be required to facilitate the stabilizing interactions of the tail.

3. Conclusion

We have reported design, chemical synthesis and biological evaluation, as FFA1 agonists, of two structurally distinct series of 1,2,4-thiadiazole-based compounds which represent an SAR-informative evolution of the earlier reported FFA1 agonists. One of the series (**4a-t**) is structurally related to classical FFA1 agonist GW9508 and has delivered compounds of low micromolar. Moreover, counter-screening of these compounds against other free fatty acid receptors (FFA2-4) confirmed **4a-t** to be selective agonists of FFA1 as no activation of FFA2-4 was observed at 10 μM concentration. The other series (**5a-q**) was designed as a truncated version of the earlier reported series **3**. However, contrary to the expectations, the compounds **5a-q** turned out to be inactive. With the structural understanding of this phenomenon gained through in silico docking into the crystal structure of FFA1, this sets important boundaries to the periphery design of FFA1 agonists.

4. Experimental protocols

All reactions were conducted in oven-dried glassware in atmosphere of nitrogen. Melting points were measured with a Buchi B-520 melting point apparatus and were not corrected. Analytical thin-layer chromatography was carried out on Silufol UV-254 silica gel plates using appropriate mixtures of ethyl acetate and hexane. Compounds were visualized with short-wavelength UV light. ^{1}H NMR and ^{13}C NMR spectra were recorded on Bruker MSL-300 spectrometers in DMSO-D6-d_6 using TMS as an internal standard. Mass spectra were recorded using Shimadzu LCMS-2020 system with electron impact (EI) ionization. All and reagents and solvents were obtained from commercial sources and used without purification.

4.1 Synthesis

*4.1.1. tert-Butyl 3-(4-{[hydrazinyl(thioxo)acetyl]amino}phenyl)propanoate (**7**)*

tert-Butyl 3-(4-aminophenyl)propanoate (1,105 mg, 5.0 mmol) was dissolved in THF (25 mL). Triethylamine (0.765 mL, 5.5 mmol) and chloroacetyl chloride (0.4 mL, 5.0 mmol) were added and the reaction mixture was stirred at room temperature for 16 h. The precipitate of triethylammonium chloride was filtered off and the fitrate concentrated in vacuo. The crude tert-butyl 3-{4-[(chloroacetyl)amino]phenyl}propanoate thus obtained was judged by ^{1}H NMR to be sufficiently pure to be used in the next step without further purification.

To a suspension of elementary sulfur (512 mg, 16.0 mmol) in dry DMF (20 mL) was sequentially added (in dropwise fashion) triethylamine (2.25 mL, 16.0 mmol), morpholine (90 μL, 1.06 mmol) and the resulting mixture was stirred for 30 min. It was treated with a solution of tert-butyl 3-{4-[(chloroacetyl)amino]phenyl}propanoate (1.5 g, 0.5 mmol) in DMF (5 mL). The resulting mixture was stirred overnight, poured into water (50 mL) and the resulting precipitate was separated by filtration and air-dried. It was suspended in acetone (50mL) and the insoluble residue of excess unreacted sulfur was filtered off and discarded. The filtrate was evaporated to dryness and the residue was dissolved in dry DMF (15 mL), treated with hydrazine hydrate (2.5 mL) and stirred for 12 hours. The reaction mixture was poured into water; the pH of the aqueous medium was adjusted to 5.0 with 2M aqueous HCl. The precipitate formed was filtered off and air dried to provide the title compounds (0.72 g, 45% over three steps) as yellow solid: m.p. 176-180 °C. ^{1}H NMR (300 MHz, DMSO-d_6) δ ppm 10.16 (br s, 1H), 7.67 – 7.61 (m, 2H), 7.24 – 7.18 (m, 2H), 2.84 – 2.74 (m, 2H), 2.57 – 2.51 (m, 2H), 1.36 (s, 9H); ^{13}C NMR (75 MHz, DMSO-d_6) δ ppm 71.5, 166.9, 158.0, 136.8, 135.5, 128.6, 119.9, 36.2, 34.3, 27.7; MS *m/z* 324.5 ($M+H^+$).

*4.1.2. General procedure for the preparation of compounds **4a-u** and **5a-q***

To a solution of the respective carboxylic acid (**8a-u** or **9**, 0.5 mmol) in DCM (4 mL) carbonyl-1,1′-diimidazole (0.55 mmol, 90 mg) was added and the mixture was stirred at r. t. for 30 min. To the resulting solution of the carboxylic acid imidazolide, respective thiohydrazide (**7** or **10a-q**) was added and the reaction mixture was stirred at r. t. for 16 h. The solvent was removed *in vacuo*, the residue was dissolved in glacial acetic acid (3 mL) and the solution was heated at reflux for 30 min. It was then cooled down to r. t., poured into water (50 mL), the resulting precipitate was collected by filtration and dried *in vacuo*. It was then combined with 4M solution of HCl in 1,4-dioxane (5 mL); the mixture was stirred at r. t. for 16 h and poured into water (50 mL). The precipitate was collected by filtration, washed with water and air-dried to provide the title compounds in yields indicated.

*4.1.2.1. 3-{4-[({5-[(4-Fluorophenoxy)methyl]-1,3,4-thiadiazol-2-yl}carbonyl)amino]phenyl}propanoic acid (**4a**)*

White solid, m.p. 160-165 °C, yield 56 %; ^{1}H NMR (300 MHz, DMSO-d_6) δ ppm 11.10 (s, 1H), 7.73 (d, J = 8.4 Hz, 2H), 7.23 (d, J = 8.4 Hz, 2H), 7.19 – 7.10 (m, 4H), 5.66 (s, 2H), 2.81 (t, J = 7.5 Hz, 2H), 2.54 (t, J = 7.5 Hz, 2H); ^{13}C NMR (75 MHz, DMSO-d_6) δ ppm 173.6, 171.1, 166.8, 155.8, 153.4, 137.3, 135.5, 128.4, 120.8, 64.8, 35.1, 29.8; MS *m/z* 402.5 ($M+H^+$); HRMS (ESI), *m/z* calcd for $C_{19}H_{17}FN_3O_4S$ [$M+H^+$] 402.0924, found 402.0918.

*4.1.2.2. 3-{4-[({5-[(2,5-Dimethylphenoxy)methyl]-1,3,4-thiadiazol-2-yl}carbonyl)amino]phenyl}propanoic acid (**4b**)*

White solid, m.p. 155-157 °C, yield 42 %; ^{1}H NMR (300 MHz, DMSO-d_6) δ ppm 12.07 (br s, 1H), 11.10 (s, 1H), 7.73 (d, *J* = 8.3 Hz, 2H), 7.23 (d, *J* = 8.3 Hz, 2H), 7.07 (d, *J* = 7.5 Hz, 1H), 6.97 (s, 1H), 6.75 (d, *J* = 7.4 Hz, 1H), 5.65 (s, 2H), 2.81 (t, *J* = 7.5 Hz, 2H), 2.54 (t, *J* = 7.5 Hz, 2H), 2.28 (s, 3H), 2.18 (s, 3H); ^{13}C NMR (75 MHz, DMSO-d_6) δ ppm 173.6, 172.0, 166.6, 155.8, 155.1, 137.3, 136.3, 135.5, 130.4, 128.4, 122.8, 122.0, 120.8, 112.9, 64.4, 35.1, 29.8, 20.9, 15.4; MS *m/z* 412.5 ($M+H^+$); HRMS (ESI), *m/z* calcd for $C_{21}H_{21}NaN_3O_4S$ [$M+Na^+$] 434.1150, found 434.1145.

*4.1.2.3. 3-{4-[({5-((2,3-Dihydro-1H-inden-6-yloxy)methyl)-1,3,4-thiadiazol-2-yl}carbonyl)amino]phenyl}propanoic acid (**4c**)*

White solid, m.p. 168-171 °C, yield 48 %; ^{1}H NMR (300 MHz, DMSO-d_6) δ ppm 12.1 (br s, 1H), 11.15 (s, 1H), 7.73 (d, *J* = 8.4 Hz, 2H), 7.23 (d, *J* = 8.4 Hz, 2H), 7.15 (d, *J* = 8.2 Hz, 1H), 6.98 (s, 1H), 6.84 (dd, *J* = 8.2, 2.2 Hz, 1H), 5.63 (s, 2H), 2.89 – 2.73 (m, 6H), 2.54 (t, *J* = 7.5 Hz, 2H), 2.00 (t, *J* = 7.5 Hz, 2H); ^{13}C NMR (75 MHz, DMSO-d_6) δ ppm 173.4, 171.5, 166.5, 155.9, 155.7, 145.3, 137.2, 136.8, 135.4, 128.3, 124.6, 120.7, 113.0, 111.0, 64.4, 35.0, 32.4, 31.2, 29.7, 25.1; MS *m/z* 424.5 ($M+H^+$); HRMS (ESI), *m/z* calcd for $C_{22}H_{22}N_3O_4S$ [$M+H^+$] 424.1331, found 424.1326.

*4.1.2.4. 3-{4-[({5-[(3-Chlorophenoxy)methyl]-1,3,4-thiadiazol-2-yl}carbonyl)amino]phenyl}propanoic acid (**4d**)*

White solid, m.p. 162-165 °C, yield 45 %; ^{1}H NMR (300 MHz, DMSO-d_6) δ ppm 12.09 (br s, 1H), 11.11 (s, 1H), 7.73 (d, *J* = 8.4 Hz, 2H), 7.37 (t, *J* = 8.2 Hz, 1H), 7.28 – 7.20 (m, 3H), 7.09 (dd, *J* = 8.1, 2.1 Hz, 2H), 5.72 (s, 2H), 2.81 (t, *J* = 7.5 Hz, 2H), 2.54 (t, *J* = 7.5 Hz, 2H); ^{13}C NMR (75 MHz, DMSO-d_6) δ ppm 173.6, 170.6, 166.9, 158.0, 155.7, 137.3, 135.6, 133.8, 131.0, 128.6, 128.4, 121.8, 120.8, 115.1, 114.1, 64.4, 35.1, 29.8; MS *m/z* 419.0 ($M+H^+$); HRMS (ESI), *m/z* calcd for $C_{19}H_{17}ClN_3O_4S$ [$M+H^+$] 418.0628, found 418.0623.

*4.1.2.5. 3-{4-[({5-[(3,4-Dimethylphenoxy)methyl]-1,3,4-thiadiazol-2-yl}carbonyl)amino]phenyl}propanoic acid (**4e**)*

White solid, m.p. 155-158 °C, yield 42 %; ^{1}H NMR (300 MHz, DMSO-d_6) δ ppm 11.10 (s, 1H), 7.73 (d, *J* = 8.2 Hz, 2H), 7.23 (d, *J* = 8.2 Hz, 2H), 7.00 (d, *J* = 7.1 Hz, 1H), 5.63 (s, 2H), 2.81 (t, *J* = 7.5 Hz, 2H), 2.53 (t, *J* = 7.5 Hz, 2H), 2.22 (s, 3H), 2.19 (s, 3H); ^{13}C NMR (75 MHz, DMSO-

d$_6$) δ ppm 173.6, 172.1, 166.6, 155.8, 153.1, 137.3, 135.5, 131.4, 130.3, 128.4, 127.1, 125.8, 120.8, 112.1, 64.6, 35.1, 29.8, 20.0, 15.8; MS *m/z* 412.5 (M+H$^+$); HRMS (ESI), *m/z* calcd for $C_{21}H_{22}N_3O_4S$ [M+H$^+$] 412.1331, found 412.1326.

*4.1.2.6. 3-{4-[({5-[(2,4-Dimethylphenoxy)methyl]-1,3,4-thiadiazol-2-yl}carbonyl)amino]phenyl}propanoic acid (**4f**)*

White solid, m.p. 160-163 °C, yield 39 %; ^{1}H NMR (300 MHz, DMSO-*d*$_6$) δ ppm 11.09 (s, 1H), 7.72 (d, *J* = 8.3 Hz, 2H), 7.23 (d, *J* = 8.3 Hz, 2H), 7.07 (d, *J* = 8.2 Hz, 1H), 6.91 (s, 1H), 6.82 (d, *J* = 8.1 Hz, 1H), 5.62 (s, 2H), 2.81 (t, *J* = 7.5 Hz, 2H), 2.53 (t, *J* = 7.5 Hz, 2H), 2.20 (s, 3H), 2.15 (s, 3H); ^{13}C NMR (75 MHz, DMSO-*d*$_6$) δ ppm 173.6, 171.6, 166.6, 155.8, 155.1, 137.6, 137.3, 135.5, 130.2, 129.4, 128.4, 120.8, 116.4, 111.9, 64.2, 35.1, 29.8, 19.5, 18.3; MS *m/z* 412.5 (M+H$^+$); HRMS (ESI), *m/z* calcd for $C_{21}H_{21}NaN_3O_4S$ [M+Na$^+$] 434.1150, found 434.1145.

*4.1.2.7. 3-(4-{[(5-{[3-(Trifluoromethyl)phenoxy]methyl}-1,3,4-thiadiazol-2-yl)carbonyl]amino}phenyl)propanoic acid (**4g**)*

White solid, m.p. 152-154 °C, yield 44 %; ^{1}H NMR (300 MHz, DMSO-*d*$_6$) δ ppm 12.07 (br s, 1H), 11.11 (s, 1H), 7.73 (d, *J* = 8.3 Hz, 2H), 7.59 (t, *J* = 7.9 Hz, 1H), 7.50 – 7.35 (m, 3H), 7.23 (d, *J* = 8.3 Hz, 2H), 5.80 (s, 2H), 2.81 (t, *J* = 7.5 Hz, 2H), 2.54 (t, *J* = 7.5 Hz, 2H); ^{13}C NMR (75 MHz, DMSO-*d*$_6$) δ ppm 173.7, 170.5, 167.0, 157.5, 155.8, 137.4, 135.6, 130.9, 130.4 (q, *J* = 32.0 Hz), 128.5, 123.9 (q, *J* = 272.6 Hz), 120.8, 119.4, 118.4 (q, *J* = 3.7 Hz), 111.7 (q, *J* = 3.6 Hz), 64.5, 35.2, 29.8; MS *m/z* 452.5 (M+H$^+$); HRMS (ESI), *m/z* calcd for $C_{20}H_{17}F_3N_3O_4S$ [M+H$^+$] 452.0892, found 452.0886.

*4.1.2.8. 3-{4-[({5-[(3-Methylphenoxy)methyl]-1,3,4-thiadiazol-2-yl}carbonyl)amino]phenyl}propanoic acid (**4h**)*

White solid, m.p. 195-197 °C, yield 40 %; ^{1}H NMR (300 MHz, DMSO-*d*$_6$) δ ppm 12.14 (br s, 1H), 11.15 (s, 1H), 7.73 (d, *J* = 8.4 Hz, 2H), 7.30 – 7.17 (m, 3H), 6.98 – 6.81 (m, 3H), 5.66 (s, 2H), 2.80 (t, *J* = 7.5 Hz, 2H), 2.54 (t, *J* = 7.5 Hz, 2H), 2.29 (s, 3H); ^{13}C NMR (75 MHz, DMSO-*d*$_6$) δ ppm 73.6, 171.4, 166.7, 157.1, 155.8, 139.3, 137.3, 135.5, 129.3, 128.4, 122.5, 120.8, 115.7, 111.9, 64.1, 35.1, 29.8, 20.9; MS *m/z* 398.5 (M+H$^+$); HRMS (ESI), *m/z* calcd for $C_{20}H_{20}N_3O_4S$ [M+H$^+$] 398.1174, found 398.1169.

*4.1.2.9. 3-{4-[({5-[(4-Ethylphenoxy)methyl]-1,3,4-thiadiazol-2-yl}carbonyl)amino]phenyl}propanoic acid (**4i**)*

White solid, m.p. 168-170 °C, yield 48 %; ^{1}H NMR (300 MHz, DMSO-d_6) δ ppm 12.06 (br s, 1H), 11.09 (s, 1H), 7.73 (d, *J* = 8.2 Hz, 2H), 7.23 (d, *J* = 8.2 Hz, 2H), 7.16 (d, *J* = 8.3 Hz, 2H), 7.01 (d, *J* = 8.3 Hz, 2H), 5.64 (s, 2H), 2.80 (t, *J* = 7.5 Hz, 2H), 2.57 (t, *J* = 7.5 Hz, 2H), 2.53 (d, *J* = 3.2 Hz, 2H), 1.15 (t, *J* = 7.6 Hz, 3H); ^{13}C NMR (75 MHz, DMSO) δ ppm 173.61, 171.52, 166.69, 155.77, 155.13, 137.32, 137.16, 135.52, 128.77, 128.43, 120.79, 114.92, 64.29, 35.13, 29.78, 27.20, 15.72; MS *m/z* 412.5 (M+H+); HRMS (ESI), *m/z* calcd for $C_{21}H_{22}N_3O_4S$ [M+H$^+$] 412.1331, found 412.1326.

*4.1.2.10. 3-{4-[({5-[(4-Methylphenoxy)methyl]-1,3,4-thiadiazol-2-yl}carbonyl)amino]phenyl}propanoic acid (**4j**)*

White solid, m.p. 211-214 °C, yield 43 %; ^{1}H NMR (300 MHz, DMSO-d_6) δ ppm 11.10 (s, 1H), 7.73 (d, *J* = 8.4 Hz, 2H), 7.23 (d, *J* = 8.4 Hz, 2H), 7.14 (d, *J* = 8.4 Hz, 2H), 6.99 (d, *J* = 8.5 Hz, 2H), 5.64 (s, 2H), 2.81 (t, *J* = 7.5 Hz, 2H), 2.54 (t, *J* = 7.5 Hz, 2H), 2.25 (s, 3H); ^{13}C NMR (75 MHz, DMSO-d_6) δ ppm 173.6, 171.5, 166.7, 155.8, 155.0, 137.3, 135.5, 130.7, 129.9, 128.4, 120.8, 114.9, 64.3, 35.1, 29.8, 20.0; MS *m/z* 398.5 (M+H+); HRMS (ESI), *m/z* calcd for $C_{20}H_{20}N_3O_4S$ [M+H$^+$] 398.1174, found 398.1169.

*4.1.2.11. 3-{4-[({5-[(4-Methoxyphenoxy)methyl]-1,3,4-thiadiazol-2-yl}carbonyl)amino]phenyl}propanoic acid (**4k**)*

White solid, m.p. 178-180 °C, yield 49 %; ^{1}H NMR (300 MHz, DMSO-d_6) δ ppm 12.15 (br s, 1H), 11.15 (s, 1H), 7.73 (d, *J* = 8.4 Hz, 2H), 7.23 (d, *J* = 8.4 Hz, 2H), 7.04 (d, *J* = 6.2 Hz, 2H), 6.90 (d, *J* = 9.1 Hz, 2H), 5.61 (s, 2H), 3.71 (s, 3H), 2.80 (t, *J* = 7.5 Hz, 2H), 2.54 (t, *J* = 7.5 Hz, 2H); ^{13}C NMR (75 MHz, DMSO-d_6) δ ppm 173.6, 171.6, 166.7, 155.8, 154.3, 151.0, 137.4, 135.5, 128.4, 120.8, 116.3, 114.7, 64.9, 55.3, 35.1, 29.8; MS *m/z* 414.5 (M+H$^+$); HRMS (ESI), *m/z* calcd for $C_{20}H_{19}NaN_3O_5S$ [M+Na$^+$] 436.0943, found 436.0938.

*4.1.2.12. 3-{4-[({5-[(2-Methylphenoxy)methyl]-1,3,4-thiadiazol-2-yl}carbonyl)amino]phenyl}propanoic acid (**4l**)*

White solid, m.p. 188-182 °C, yield 43 %; ^{1}H NMR (300 MHz, DMSO-d_6) δ ppm 12.07 (br s, 1H), 11.10 (s, 1H), 7.73 (d, *J* = 8.4 Hz, 2H), 7.27 – 7.16 (m, 5H), 7.12 (d, *J* = 8.0 Hz, 1H), 6.93 (t, *J* = 7.3 Hz, 1H), 5.67 (s, 2H), 2.81 (t, *J* = 7.5 Hz, 2H), 2.54 (t, *J* = 7.5 Hz, 2H), 2.23 (s, 3H); ^{13}C NMR (75 MHz, DMSO-d_6) δ ppm 173.6, 171.9, 166.6, 155.8, 155.2, 137.37 135.5, 130.7, 128.4, 127.0, 126.0, 121.5, 120.8, 112.1, 64.5, 35.1, 29.8, 15.8; MS *m/z* 398.5 (M+H$^+$); HRMS (ESI), *m/z* calcd for $C_{20}H_{19}NaN_3O_4S$ [M+Na$^+$] 420.0994, found 420.0988.

*4.1.2.13. 3-(4-(5-(2-(4-Chlorophenyl)-2-phenylethyl)-1,3,4-thiadiazole-2-carboxamido)phenyl)propanoic acid (**4m**)*

White solid, m.p. 220-222 °C, yield 48 %; ^{1}H NMR (300 MHz, DMSO-d_6) δ ppm 12.16 (br s, 1H), 10.98 (s, 1H), 7.71 – 7.63 (m, 2H), 7.51 – 7.39 (m, 4H), 7.39 – 7.26 (m, 4H), 7.25 – 7.14 (m, 3H), 4.60 (d, *J* = 6.1 Hz, 1H), 4.03 (d, *J* = 5.0 Hz, 2H), 2.88 – 2.71 (m, 2H), 2.52 (t, *J* = 7.5 Hz, 2H); ^{13}C NMR (75 MHz, DMSO-d_6) δ ppm 173.6, 172.6, 165.6, 155.9, 142.6, 142.1, 137.2, 135.5, 131.2, 129.5, 128.6, 128.4, 128.4, 127.6, 126.7, 120.7, 49.8, 35.1, 34.8, 29.8; MS *m/z* 493.2 (M+H$^+$); HRMS (ESI), *m/z* calcd for $C_{26}H_{23}ClN_3O_3S$ [M+H$^+$] 492.1149, found 492.1143.

*4.1.2.14. 3-(4-(5-(2-(4-Methoxyphenyl)-2-phenylethyl)-1,3,4-thiadiazole-2-carboxamido)phenyl)propanoic acid (**4n**)*

White solid, m.p. 215-217 °C, yield 45 %; ^{1}H NMR (300 MHz, DMSO-d_6) δ ppm 12.07 (br s, 1H), 10.94 (s, 1H), 7.67 (d, *J* = 8.3 Hz, 2H), 7.41 (d, *J* = 7.4 Hz, 2H), 7.38 – 7.25 (m, 4H), 7.20 (d, *J* = 8.4 Hz, 3H), 6.86 (d, *J* = 8.4 Hz, 2H), 4.50 (t, *J* = 8.1 Hz, 1H), 3.98 (d, *J* = 7.8 Hz, 2H), 3.70 (s, 3H), 2.79 (t, *J* = 7.5 Hz, 2H), 2.53 (t, *J* = 7.5 Hz, 2H); ^{13}C NMR (75 MHz, DMSO-d_6) δ ppm 173.6, 173.0, 165.5, 157.9, 155.9, 143.5, 137.2, 135.5, 134.9, 128.7, 128.4, 128.4, 127.5, 126.4, 120.7, 113.9, 54.9, 49.8, 35.2, 35.1, 29.8; MS *m/z* 488.5 (M+H$^+$); HRMS (ESI), *m/z* calcd for $C_{27}H_{26}N_3O_4S$ [M+H$^+$] 488.1644, found 488.1639.

*4.1.2.15. 3-(4-(5-(2-(2-Fluorophenyl)-2-phenylethyl)-1,3,4-thiadiazole-2-carboxamido)phenyl)propanoic acid (**4o**)*

White solid, m.p. 232-234 °C, yield 47 %; ^{1}H NMR (300 MHz, DMSO-d_6) δ ppm 10.98 (s, 1H), 7.70 – 7.61 (m, 3H), 7.40 (d, *J* = 7.6 Hz, 2H), 7.31 (d, *J* = 7.5 Hz, 2H), 7.29 – 7.09 (m, 6H), 4.85 (t, *J* = 8.2 Hz, 1H), 4.05 (d, *J* = 8.2 Hz, 2H), 2.79 (t, *J* = 7.5 Hz, 2H), 2.53 (t, *J* = 7.5 Hz, 2H); ^{13}C NMR (75 MHz, DMSO-d_6) δ ppm 173.6, 172.5, 165.7, 159.8 (d, *J* = 244.4 Hz), 155.9, 141.7, 137.2, 135.5, 129.5 (d, *J* = 14.0 Hz), 128.8 (d, *J* = 4.0 Hz), 128.7 (d, *J* = 8.5 Hz), 128.5, 128.4, 127.7, 126.8, 120.7, 124.6 (d, *J* = 3.4 Hz), 115.5 (d, *J* = 22.3 Hz), 43.3, 43.3, 35.1, 34.1, 29.8; MS *m/z* 476.5 (M+H$^+$); HRMS (ESI), *m/z* calcd for $C_{26}H_{23}FN_3O_3S$ [M+H$^+$] 476.1444, found 476.1439.

*4.1.2.16. 3-(4-(5-(2-(Benzo[d][1,3]dioxol-6-yl)-2-phenylethyl)-1,3,4-thiadiazole-2-carboxamido)phenyl)propanoic acid (**4p**)*

White solid, m.p. 212-214 °C, yield 42 %; ^{1}H NMR (300 MHz, DMSO-d_6) δ ppm 12.06 (br s, 1H), 10.94 (s, 1H), 7.67 (d, *J* = 7.9 Hz, 2H), 7.43 (d, *J* = 7.1 Hz, 2H), 7.29 (t, *J* = 7.1 Hz, 2H),

7.20 (d, *J* = 7.8 Hz, 3H), 7.07 (s, 1H), 6.85 (dd, *J* = 23.6, 7.8 Hz, 2H), 5.95 (d, *J* = 4.4 Hz, 2H), 4.48 (t, *J* = 7.8 Hz, 1H), 4.03 – 3.93 (m, 2H), 2.79 (t, *J* = 7.5 Hz, 2H), 2.52 (t, *J* = 7.5 Hz, 2H); ^{13}C NMR (75 MHz, DMSO-d_6) δ ppm 173.6, 172.9, 165.5, 155.9, 147.4, 145.8, 143.3, 137.2, 136.9, 135.5, 128.4, 128.4, 127.5, 126.5, 120.9, 120.7, 108.1, 108.0, 100.8, 50.2, 35.1, 35.0, 29.7; MS *m/z* 502.5 ($M+H^+$); HRMS (ESI), *m/z* calcd for $C_{27}H_{24}N_3O_5S$ [$M+H^+$] 502.1437, found 502.1431.

*4.1.2.17. 3-(4-{[(5-Benzyl-1,3,4-thiadiazol-2-yl)carbonyl]amino}phenyl)propanoic acid (**4q**)*

White solid, m.p. 155-257 °C, yield 51 %; ^{1}H NMR (300 MHz, DMSO-d_6) δ ppm 12.11 (br s, 1H), 11.05 (s, 1H), 7.71 (d, *J* = 8.5 Hz, 2H), 7.38 (d, *J* = 4.6 Hz, 2H), 7.36 – 7.27 (m, 2H), 7.21 (d, *J* = 8.5 Hz, 2H), 4.56 (s, 2H), 2.79 (t, *J* = 7.5 Hz, 2H), 2.53 (t, *J* = 7.5 Hz, 2H); ^{13}C NMR (75 MHz, DMSO-d_6) δ ppm 174.2, 173.6, 166.2, 155.9, 137.3, 137.2, 135.6, 128.8, 128.8, 128.4, 127.2, 120.7, 35.1, 29.8; MS *m/z* 368.5 ($M+H^+$); HRMS (ESI), *m/z* calcd for $C_{19}H_{18}N_3O_3S$ [$M+H^+$] 368.1069, found 368.1063.

*4.1.2.18. 3-[4-({[5-(3-Chlorobenzyl)-1,3,4-thiadiazol-2-yl]carbonyl}amino)phenyl]propanoic acid (**4r**)*

White solid, m.p. 161-163 °C, yield 48 %; ^{1}H NMR (300 MHz, DMSO-d_6) δ ppm 11.01 (s, 1H), 7.71 (d, *J* = 8.5 Hz, 2H), 7.49 (s, 1H), 7.42 – 7.33 (m, 3H), 7.22 (d, *J* = 8.5 Hz, 2H), 4.60 (s, 2H), 2.80 (t, *J* = 7.5 Hz, 2H), 2.53 (t, *J* = 7.5 Hz, 2H); ^{13}C NMR (75 MHz, DMSO-d_6) δ ppm 173.7, 173.3, 166.4, 155.9, 139.7, 137.3, 135.6, 133.3, 130.7, 128.8, 128.5, 127.6, 127.3, 120.8, 35.2, 34.6, 29.8; MS *m/z* 403.0 ($M+H^+$); HRMS (ESI), *m/z* calcd for $C_{19}H_{17}ClN_3O_3S$ [$M+H^+$] 402.0679, found 402.0674.

*4.1.2.19. 3-[4-({[5-(3-Fluorobenzyl)-1,3,4-thiadiazol-2-yl]carbonyl}amino)phenyl]propanoic acid (**4s**)*

White solid, m.p. 175-177 °C, yield 46 %; ^{1}H NMR (300 MHz, DMSO-d_6) δ ppm 12.07 (br s, 1H), 11.03 (s, 1H), 7.71 (d, *J* = 7.9 Hz, 2H), 7.43 (dd, *J* = 14.4, 7.2 Hz, 1H), 7.31 – 7.19 (m, 2H), 7.14 (t, *J* = 8.6 Hz, 1H), 4.61 (s, 2H), 2.80 (t, *J* = 7.5 Hz, 2H), 2.53 (t, *J* = 7.5 Hz, 2H); ^{13}C NMR (75 MHz, DMSO-d_6) δ ppm 173.6, 173.3, 166.3, 162.1 (d, *J* = 244.2 Hz), 155.9, 139.8 (d, *J* = 7.7 Hz), 137.2, 135.5, 130.7 (d, *J* = 8.4 Hz), 128.4, 125.0 (d, *J* = 2.6 Hz), 120.8, 115.7 (d, *J* = 21.8 Hz), 114.1 (d, *J* = 20.8 Hz), 35.1, 34.7, 29.8; MS *m/z* 386.5 ($M+H^+$); HRMS (ESI), *m/z* calcd for $C_{19}H_{16}NaFN_3O_3S$ [$M+Na^+$] 408.0794, found 408.0789.

*4.1.2.20. 3-[4-({[5-(4-Chlorobenzyl)-1,3,4-thiadiazol-2-yl]carbonyl}amino)phenyl]propanoic acid (**4t**)*

White solid, m.p. 181-183 °C, yield 42 %; ^{1}H NMR (300 MHz, DMSO-d_6) δ ppm 11.02 (s, 1H), 7.71 (d, *J* = 8.4 Hz, 2H), 7.42 (s, 2H), 7.25 – 7.19 (m, 2H), 4.58 (s, 2H), 2.80 (t, *J* = 7.5 Hz, 2H), 2.53 (t, *J* = 7.5 Hz, 2H); ^{13}C NMR (75 MHz, DMSO-d_6) δ ppm 173.8, 173.8, 166.4, 155.9, 137.3, 136.3, 135.6, 132.0, 130.8, 128.8, 128.5, 120.8, 35.5, 34.4, 29.8; MS *m/z* 402.8 ($M+H^+$); HRMS (ESI), *m/z* calcd for $C_{19}H_{17}ClN_3O_3S$ [$M+H^+$] 402.0679, found 402.0674.

*4.1.2.21. [4-({5-[(2-Methoxy-5-methylphenyl)carbamoyl]-1,3,4-thiadiazol-2-yl}methyl)phenoxy]acetic acid (**5a**)*

White solid, m.p. 167-170 °C, yield 47 %; ^{1}H NMR (300 MHz, DMSO-d_6) δ ppm 13.05 (br s, 1H), 9.79 (s, 1H), 7.87 (s, 1H), 7.30 (d, *J* = 8.5 Hz, 2H), 7.06 – 6.96 (m, 2H), 6.90 (d, *J* = 8.6 Hz, 2H), 4.67 (s, 2H), 4.48 (s, 2H), 3.86 (s, 3H), 2.26 (s, 3H); ^{13}C NMR (75 MHz, DMSO-d_6) δ ppm 175.3, 170.0, 165.6, 156.9, 155.1, 147.5, 129.9, 129.7, 129.4, 125.9, 125.3, 121.5, 114.8, 111.2, 64.5, 56.0, 34.4, 20.4; MS *m/z* 414.5 ($M+H^+$).

*4.1.2.22. [4-({5-[(2,4-Difluorophenyl)carbamoyl]-1,3,4-thiadiazol-2-yl}methyl)phenoxy]acetic acid (**5b**)*

White solid, m.p. 169-172 °C, yield 67 %; ^{1}H NMR (300 MHz, DMSO-d_6) δ ppm 12.90 (s, 1H), 10.89 (s, 1H), 7.57 (td, J = 8.8, 6.3 Hz, 1H), 7.44 – 7.34 (m, 1H), 7.30 (d, *J* = 8.6 Hz, 2H), 7.18 – 7.07 (m, 1H), 6.90 (d, *J* = 8.6 Hz, 2H), 4.66 (s, 2H), 4.49 (s, 2H); ^{13}C NMR (75 MHz, DMSO-d_6) δ ppm 175.3, 170.2, 165.1, 160.2 (dd, *J* = 245.7, 11.7 Hz), 157.0, 156.6, 156.2 (dd, *J* = 251.0, 12.9 Hz), 130.0, 129.8, 128.6 (dd, *J* = 10.3, 1.9 Hz), 120.8 (dd, *J* = 12.7, 3.8 Hz),114.8, 111.5 (dd, *J* = 22.2, 3.6 Hz), 104.6 (dd, *J* = 26.7, 24.5 Hz), 64.4, 34.4; MS *m/z* 406.2 ($M+H^+$).

*4.1.2.23. [4-({5-[(4-Methylphenyl)carbamoyl]-1,3,4-thiadiazol-2-yl}methyl)phenoxy]acetic acid (**5c**)*

White solid, m.p. 195-199 °C, yield 52 %; ^{1}H NMR (300 MHz, DMSO-d_6) δ ppm 13.01 (br s, 1H), 11.03 (s, 1H), 7.69 (d, *J* = 8.4 Hz, 2H), 7.30 (d, *J* = 8.6 Hz, 2H), 7.16 (d, *J* = 8.4 Hz, 2H), 6.90 (d, *J* = 8.6 Hz, 2H), 4.66 (s, 2H), 4.48 (s, 2H), 2.27 (s, 3H); ^{13}C NMR (75 MHz, DMSO-d_6) δ ppm 175.0, 170.2, 166.2, 157.0, 156.0, 135.2, 133.8, 130.0, 129.8, 129.1, 120.7, 114.8, 64.4, 34.4, 20.5; MS *m/z* 384.5 ($M+H^+$).

*4.1.2.24. [4-({5-[(2-Fluorophenyl)carbamoyl]-1,3,4-thiadiazol-2-yl}methyl)phenoxy]acetic acid (**5d**)*

White solid, m.p. 218-220 °C, yield 83 %; ^{1}H NMR (300 MHz, DMSO-d_6) δ ppm 12.99 (br s, 1H), 10.83 (s, 1H), 7.59 (t, *J* = 7.8 Hz, 1H), 7.36 – 7.27 (m, 4H), 7.26 – 7.19 (m, 1H), 6.91 (d, *J* = 8.6 Hz, 2H), 4.66 (s, 2H), 4.49 (s, 2H); ^{13}C NMR (75 MHz, DMSO-d_6) δ ppm 174.9, 169.9, 165.0, 156.9, 156.2, 155.5 (d, *J* = 247.8 Hz), 129.8, 129.7, 127.6 (d, *J* = 7.8 Hz), 126.6 (d, *J* = 1.1 Hz), 124.3 (d, *J* = 3.7 Hz), 124.1 (d, *J* = 12.2 Hz), 115.8 (d, *J* = 19.7 Hz), 114.8, 64.5, 34.36; MS *m/z* 388.5 ($M+H^+$).

*4.1.2.25. [4-({5-[(3-Methylphenyl)carbamoyl]-1,3,4-thiadiazol-2-yl}methyl)phenoxy]acetic acid (**5e**)*

White solid, m.p. 210-212 °C, yield 44 %; ^{1}H NMR (300 MHz, DMSO-d_6) δ ppm 13.00 (br s, 1H), 11.00 (s, 1H), 7.67 (s, 1H), 7.59 (d, *J* = 8.2 Hz, 1H), 7.30 (d, *J* = 8.6 Hz, 2H), 7.24 (t, *J* = 7.8 Hz, 1H), 6.97 (d, *J* = 7.5 Hz, 1H), 6.91 (d, *J* = 8.6 Hz, 2H), 4.66 (s, 2H), 4.48 (s, 2H), 2.30 (s, *J* = 9.2 Hz, 3H); ^{13}C NMR (75 MHz, DMSO-d_6) δ ppm 175.0, 170.1, 166.1, 156.9, 156.1, 138.0, 137.5, 129.9, 129.8, 128.5, 125.3, 121.2, 118.0, 114.8, 64.5, 34.4, 21.1; MS *m/z* 384.5 ($M+H^+$).

*4.1.2.26. [4-({5-[(4-Fluorophenyl)carbamoyl]-1,3,4-thiadiazol-2-yl}methyl)phenoxy]acetic acid (**5f**)*

White solid, m.p. 216-219 °C, yield 60 %; ^{1}H NMR (300 MHz, DMSO-d_6) δ ppm 13.01 (br s, 1H), 11.20 (s, 1H), 7.89 – 7.80 (m, 2H), 7.30 (d, *J* = 8.6 Hz, 2H), 7.21 (t, *J* = 8.9 Hz, 2H), 6.91 (d, *J* = 8.6 Hz, 2H), 4.67 (s, 2H), 4.49 (s, 2H); ^{13}C NMR (75 MHz, DMSO-d_6) δ ppm 175.0, 170.0, 165.9, 158.8 (d, *J* = 241.5 Hz), 156.9, 156.1, 134.0 (d, *J* = 2.7 Hz), 129.9, 129.8, 122.6 (d, *J* = 8.0 Hz), 115.3 (d, *J* = 22.4 Hz), 114.8, 64.4, 34.4; MS *m/z* 388.4 ($M+H^+$).

*4.1.2.27. [4-({5-[(4-Chlorophenyl)carbamoyl]-1,3,4-thiadiazol-2-yl}methyl)phenoxy]acetic acid (**5g**)*

White solid, m.p. 222-224 °C, yield 83 %; ^{1}H NMR (300 MHz, DMSO-d_6) δ ppm 13.00 (br s, 1H), 11.26 (s, 1H), 7.86 (d, *J* = 8.9 Hz, 2H), 7.43 (d, *J* = 8.9 Hz, 2H), 7.30 (d, *J* = 8.6 Hz, 2H), 6.91 (d, *J* = 8.6 Hz, 2H), 4.66 (s, 2H), 4.49 (s, 2H); ^{13}C NMR (75 MHz, DMSO-d_6) δ ppm 175.1, 170.1, 165.8, 157.0, 156.3, 136.6, 129.9, 129.8, 128.6, 128.4, 122.3, 114.8, 64.5, 34.4; MS *m/z* 404.5 ($M+H^+$).

*4.1.2.28. [4-({5-[(3-Methoxyphenyl)carbamoyl]-1,3,4-thiadiazol-2-yl}methyl)phenoxy]acetic acid (**5h**)*

White solid, m.p. 193-195 °C, yield 63 %; ^{1}H NMR (300 MHz, DMSO-d_6) δ ppm 3.01 (s, 1H), 11.07 (s, 1H), 7.49 (t, *J* = 2.1 Hz, 1H); 7.44 (d, *J* = 8.1 Hz, 2H), 7.33 – 7.23 (m, 3H), 6.91 (d, *J* = 8.6 Hz, 2H), 6.73 (dd, *J* = 8.2, 2.3 Hz, 1H), 4.67 (s, 2H), 4.49 (s, 2H), 3.74 (s, 3H); ^{13}C NMR (75 MHz, DMSO-d_6) δ ppm 175.0, 170.0, 166.0, 159.4, 156.9, 156.1, 138.8, 129.9, 129.7, 129.5, 114.8, 112.9, 110.1, 106.6, 64.4, 55.0, 34.4; MS *m/z* 400.5 ($M+H^+$).

*4.1.2.29. [4-({5-[(3,4-Difluorophenyl)carbamoyl]-1,3,4-thiadiazol-2-yl}methyl)phenoxy]acetic acid (**5i**)*

White solid, m.p. 223-226 °C, yield 56 %; ^{1}H NMR (300 MHz, DMSO-d_6) δ ppm 13.01 (br s, 1H), 11.37 (s, 1H), 7.93 (ddd, *J* = 13.0, 7.4, 2.4 Hz, 2H); 7.71 – 7.63 (m, 1H), 7.46 (dd, *J* = 19.6, 9.3 Hz, 1H), 7.30 (d, *J* = 8.6 Hz, 2H), 6.91 (d, *J* = 8.6 Hz, 2H), 4.67 (s, 2H), 4.49 (s, 2H); ^{13}C NMR (75 MHz, DMSO-d_6) δ ppm 175.2, 170.0, 165.6, 156.9, 156.3, 149.0 (dd, *J* = 201.9, 12.9 Hz), 145.8 (dd, *J* = 201.6, 12.9 Hz), 134.6 (dd, *J* = 9.0, 3.0 Hz), 129.9, 129.7, 117.4 (d, *J* = 18.5 Hz), 117.2 (dd, *J* = 3.4, 2.7 Hz), 114.8, 109.8 (d, *J* = 21.7 Hz), 64.4, 34.4; MS *m/z* 406.5 ($M+H^+$).

*4.1.2.30. [4-({5-[(3,4-Dimethylphenyl)carbamoyl]-1,3,4-thiadiazol-2-yl}methyl)phenoxy]acetic acid (**5j**)*

White solid, m.p. 211-213 °C, yield 89 %; ^{1}H NMR (300 MHz, DMSO-d_6) δ ppm 12.96 (br s, 1H), 10.88 (s, 1H), 7.60 (s, 1H), 7.51 (d, *J* = 8.1 Hz, 1H), 7.30 (d, *J* = 8.6 Hz, 2H), 7.10 (d, *J* = 8.1 Hz, 1H), 6.91 (d, J = 8.6 Hz, 2H), 4.66 (s, 2H), 4.48 (s, 2H), 2.21 (s, 3H), 2.19 (s, 3H); ^{13}C NMR (75 MHz, DMSO-d_6) δ ppm 174.8, 170.0, 166.1, 156.9, 155.8, 136.3, 135.3, 132.5, 129.9, 129.8, 129.5, 121.8, 118.2, 114.8, 64.4, 34.4, 19.6, 18.8; MS *m/z* 398.5 ($M+H^+$).

*4.1.2.31. [4-({5-[(2,3-Dimethylphenyl)carbamoyl]-1,3,4-thiadiazol-2-yl}methyl)phenoxy]acetic acid (**5k**)*

White solid, m.p. 188-192 °C, yield 40 %; ^{1}H NMR (300 MHz, DMSO-d_6) δ ppm 13.02 (br s, 1H), 10.70 (s, 1H), 7.31 (d, *J* = 8.6 Hz, 2H), 7.18 – 7.08 (m, 3H), 6.91 (d, *J* = 8.6 Hz, 2H), 4.67 (s, 2H), 4.48 (s, 2H), 2.27 (s, 3H), 2.09 (s, 3H); ^{13}C NMR (75 MHz, DMSO-d_6) δ ppm 174.8, 170.1, 165.9, 156.9, 156.4, 137.1, 134.7, 132.5, 129.9, 129.8, 128.1, 125.3, 124.4, 114.8, 64.4, 34.5, 20.0, 14.1; MS *m/z* 398.5 ($M+H^+$).

*4.1.2.32. (4-{[5-(Phenylcarbamoyl)-1,3,4-thiadiazol-2-yl]methyl}phenoxy)acetic acid (**5l**)*

White solid, m.p. 152-154 °C, yield 69 %; ^{1}H NMR (300 MHz, DMSO-d_6) δ ppm 12.99 (br s, 1H), 11.09 (s, 1H), 7.82 (d, *J* = 7.9 Hz, 2H), 7.40 – 7.28 (m, 4H), 7.16 (t, *J* = 7.4 Hz, 1H), 6.91

(d, *J* = 8.6 Hz, 2H), 4.67 (s, 2H), 4.49 (s, 2H); ^{13}C NMR (75 MHz, DMSO-d_6) δ ppm 175.1, 170.1, 166.1, 156.9, 156.2, 137.7, 130.0, 129.8, 128.7, 124.7, 120.8, 114.8, 64.4, 34.4; MS *m/z* 370.4 ($M+H^+$).

*4.1.2.33. [4-({5-[(2-Methylphenyl)carbamoyl]-1,3,4-thiadiazol-2-yl}methyl)phenoxy]acetic acid (**5m**)*

White solid, m.p. 170-173 °C, yield 76 %; ^{1}H NMR (300 MHz, DMSO-d_6) δ ppm 12.96 (br s, 1H), 10.56 (s, 1H), 7.38 (d, *J* = 6.7 Hz, 1H), 7.34 – 7.24 (m, 3H), 7.23 – 7.15 (m, 2H), 6.91 (d, *J* = 8.5 Hz, 2H), 4.66 (s, 2H), 4.49 (s, 2H), 2.24 (s, 3H); ^{13}C NMR (75 MHz, DMSO-d_6) δ ppm 175.1, 170.3, 165.9, 157.0, 156.4, 134.9, 133.6, 130.5, 130.1, 129.9, 126.7, 126.4, 126.2, 114.9, 64.5, 34.5, 17.8; MS *m/z* 384.5 ($M+H^+$).

*4.1.2.34. {4-[(5-{[3-(Ethoxycarbonyl)phenyl]carbamoyl}-1,3,4-thiadiazol-2-yl)methyl]phenoxy}acetic acid (**5n**)*

White solid, m.p. 168-170 °C, yield 74 %; ^{1}H NMR (300 MHz, DMSO-d_6) δ 12.98 (br s, 1H), 11.34 (s, 1H), 8.53 (s, 1H), 8.05 (d, *J* = 8.7 Hz, 1H), 7.74 (d, *J* = 7.8 Hz, 1H), 7.52 (t, *J* = 7.9 Hz, 1H), 7.31 (d, *J* = 8.6 Hz, 2H), 6.91 (d, *J* = 8.6 Hz, 2H), 4.66 (s, 2H), 4.50 (s, 2H), 4.32 (q, *J* = 7.1 Hz, 2H), 1.33 (t, *J* = 7.1 Hz, 3H). ^{13}C NMR (75 MHz, DMSO-d_6) δ ppm 175.1, 170.1, 165.8, 165.4, 157.0, 156.5, 138.1, 130.4, 129.9, 129.8, 129.2, 125.2, 125.2, 121.3, 114.8, 64.5, 60.9, 34.4, 14.1; MS *m/z* 442.5 ($M+H^+$).

*4.1.2.35. {4-[(5-{[4-(Ethoxycarbonyl)phenyl]carbamoyl}-1,3,4-thiadiazol-2-yl)methyl]phenoxy}acetic acid (**5o**)*

White solid, m.p. 174-178 °C, yield 87 %; ^{1}H NMR (300 MHz, DMSO-d_6) δ ppm 12.94 (br s, 1H), 11.38 (s, 1H), 8.02 – 7.93 (m, 4H), 7.31 (d, *J* = 8.6 Hz, 2H), 6.91 (d, *J* = 8.6 Hz, 2H), 4.66 (s, 2H), 4.50 (s, 2H), 4.30 (q, *J* = 7.1 Hz, 2H), 1.32 (t, *J* = 7.1 Hz, 3H); ^{13}C NMR (75 MHz, DMSO-d_6) δ ppm 175.4, 170.1, 165.7, 165.2, 157.0, 156.7, 142.0, 130.0, 130.0, 129.8, 125.6, 120.2, 114.8, 64.4, 60.6, 34.4, 14.2; MS *m/z* 442.5 ($M+H^+$).

*4.1.2.36. [4-({5-[(5-Methyl-1,3,4-thiadiazol-2-yl)carbamoyl]-1,3,4-thiadiazol-2-yl}methyl)phenoxy]acetic acid (**5p**)*

White solid, m.p. 179-181 °C, yield 38 %; ^{1}H NMR (300 MHz, DMSO-d_6) δ ppm 13.32 (br s, 1H), 7.30 (d, *J* = 8.4 Hz, 2H), 6.90 (d, *J* = 8.4 Hz, 2H), 4.66 (s, 2H), 4.48 (s, 2H), 2.63 (s, 3H); ^{13}C NMR (75 MHz, DMSO-d_6) δ ppm 175.0, 170.1, 159.7, 159.7, 159.5, 159.5, 157.0, 130.0, 129.8, 114.8, 64.5, 34.4, 15.2; MS *m/z* 392.5 ($M+H^+$).

*4.1.2.37. [4-({5-[(4-Bromophenyl)carbamoyl]-1,3,4-thiadiazol-2-yl}methyl)phenoxy]acetic acid (**5q**)*

White solid, m.p. 172-174 °C, yield 76 %; ^{1}H NMR (300 MHz, DMSO-d_6) δ ppm 12.97 (br s, 1H), 11.23 (s, 1H), 7.80 (d, *J* = 8.9 Hz, 2H), 7.56 (d, *J* = 8.9 Hz, 2H), 7.30 (d, *J* = 8.6 Hz, 2H), 6.91 (d, *J* = 8.6 Hz, 2H), 4.66 (s, 2H), 4.49 (s, 1H); ^{13}C NMR (75 MHz, DMSO-d_6) δ ppm 175.2, 170.1, 165.8, 156.9, 156.3, 137.1, 131.6, 129.9, 129.8, 122.6, 116.5, 114.8, 64.4, 34.4; MS *m/z* 449.6 ($M+H^+$).

4.2. Biological assays

CHO cells stably expressing human FFA1 (stable CHO-GPR40 line created at Enamine Ltd.) were seeded (12,500 cells/well) into 384-well black-wall, clear-bottom microtiter plates 24 h prior to assay. Cells were loaded for 1 h with dye-loading solution containing Fluo-8 AM (Abcam, ab142773), Probenecid (Sigma, P8761), Pluronic F-127 (Sigma, P2443), Tartrazine (Sigma, T0388), Amaranth (Sigma, A1016) and tested using fluorometric imaging plate reader (FLIPR Tetra® High Throughput Cellular Screening System, Molecular Devices Corp.). Maximum change in fluorescence over base line was used to determine agonist response. A potent and selective agonist for FFA1 GW9508 (Selleckchem, S8014) was tested with the test compounds as a positive control. To obtain concentration response curve data nonlinear regression with variable slope (four parameters) were fitted using GraphPad Prism version 7.03 for Windows, GraphPad Software, La Jolla California USA, www.graphpad.com. For specificity screening for possible GPR41, GPR43 and GPR120 agonism, CHO cell lines stably expressing the respective receptors (purchased from The European Collection of Cell Cultures, ECACC) were used.

4.3. Docking studies

The initial 3D structure of FFA1 was obtained from the Protein Data Bank (PDB ID: 4PHU) [25] and used for subsequent docking procedures. Protein and ligand preparation, refinement and docking was performed within Schrödinger's Maestro, version 2017-2 [26]. To prepare the FFA1 receptor for docking, hydrogens and missing atoms were added, alternate residue positions were defined and the hydrogen bonding network was further optimized by re-orientating hydroxyls, amides and imidazole rings (of histidine residues) using the Protein Preparation Wizard [27]. To validate our docking protocol, the co-crystallised TAK-875 was re-docked onto FFA1 and compared to the crystal structure orientation, with an RMSD <2.5 Å [28]. To further improve the docking performance the atomic electrostatic-potential (ESP) charges were calculated with Jaguar [29] at the level of Density Functional Theory (DFT) with the B3LYP/6-31G** basis set.

These parameters were then combined with the OPLS3 force field [30] and used throughout the docking procedure. The remaining parameters and steps for receptor grid generation, ligand preparation and docking protocols were similar to the methodology of our previous studies [13, 15, 17]. Here we utilized the MacroModel [31], LigPrep [32] and GLIDE [33] modules of Schrödinger's Maestro. Images for the molecular modelling rational were rendered in PyMol [34]. To allow the comparison of residue positions within the GPCR family, the labels of residues are shown the Ballesteros Weinstein indexing system in subscript [24].

Acknowledgements

This research was supported by the Russian Scientific Foundation (project grant 14-50-00069).

Appendix A. Supplementary data

Supplementary data related to this article can be found at http://dx.doi.org/10.1016/ejmech.xxxx.xx.xxxx.

References

[1] Y. Itoh, Y. Kawamata, M. Harada, M. Kobayashi, R. Fujii, S. Fukusumi, K. Ogi, M. Hosoya, Y. Tanaka, H. Uejima, H. Tanaka, M. Maruyama, R. Satoh, S. Okubo, H. Kizawa, H. Komatsu, F. Matsumura, Y. Noguchi, T. Shinohara, S. Hinuma, Y. Fujisawa, M. Fujino. Nature 422 (2003) 173-176.

[2] E. Defossa, M. Wagner. Bioorg. Med. Chem. Lett. 24 (2014) 2991-3000.

[3] K. R. Watterson, B. D. Hudson, T. Ulven, G. Milligan. Front. Endocrinol. 5 (2014) 137.

[4] K. Kaku, K. Enya, R. Nakaya, T. Ohira, R. Matsuno. Diabetes Obes. Metab. 17 (2015) 675-681.

[5] A. D. Mancini, V. Poitout. Diabetes Obes. Metab. 17 (2015) 622-629.

[6] K. McEuen, J. Borlak, M. Chen. Int. J. Mol. Sci. 18 (2017) 1335.

[7] Z. Weng, K. Wang, H. Li, Q. Shi. Oncotarget 6 (2015) 17031-17038.

[8] M. Chen, J. Borlak, W. Tong. Hepatology 58 (2013) 388-396.

[9] T. Maekawa, R. Hara, H. Odaka, K. Fukatsu, H. Mizufune. PCT Int. Appl. WO 2003099793A1; Chem. Abstr. 140 (2003) 951003.

[10] K. Hamamura, S. Sasaki, Y. Amano, J. Sakamoto, K. Fukatsu. PCT Int. Appl. WO 2004022551A1; Chem. Abstr. 140 (2004) 220326.

[11] T. Yasuma, N. Negoro, S. Sasaki. PCT Int. Appl. WO 2005087710 A1; Chem. Abstr. 143 (2005) 1021733.

[12] R. Rharma, M. Akerman, M. G. Cardozo, J. Houze, A.-R. Li, J. Liu, J. Liu, Z. Ma, J. C. Medina, M. J. Schmitt, Y. Sun, Y. Wang, Z. Wang, L. Zhu. PCT Int. Appl. WO 2007106469 A2; Chem. Abstr. 147 (2007) 1064386.

[13] M. Krasavin, A. Lukin, D. Bagnyukova, N. Zhurilo, I. Zahanich, S. Zozulya, J. Ihalainen, M. M. Forsberg, M. Lehtonen, J. Rautio, D. Moore, I. G. Tikhonova. Bioorg. Med. Chem. 24 (2016) 5481-5494.

[14] M. Krasavin, A. Lukin, D. Bagnyukova, N. Zhurilo, I. Zahanich, S. Zozulya. J. Enzyme Inhib. Med. Chem. 32 (2017) 29-36.

[15] M. Krasavin, A. Lukin, D. Bagnyukova, N. Zhurilo, A. Golovanov, S. Zozulya, I. Zahanich, D. Moore, I. G. Tikhonova. Eur. J. Med. Chem. 127 (2017) 357-368.

[16] M. Krasavin, A. Lukin, N. Zhurilo, A. Kovalenko, I. Zahanich, S. Zozulya. J. Enz. Inh. Med. Chem. 31 (2016) 1404-1410.

[17] M. Krasavin, A. Lukin, N. Zhurilo, A. Kovalenko, I. Zahanich, S. Zozulya, D. Moore, I. G. Tikhonova. Bioorg. Med. Chem. 24 (2016) 2954-2963.

[18] Z. Li, X. Wang, X. Xu, J. Yang, W. Xia, X. Zhou, W. Huang, H. Qian. Bioorg. Med. Chem. 23 (2015) 7158-7164.

[19] J. P. Klein, Int. Pat. Appl. WO 2014133526A1; Chem. Abstr. 161 (2014) 454204.

[20] B. B. Chen, H. Y. Chen, G. J. Gesicki, R. A. Haack, J. W. Malecha, T. D. Penning, J. G. Rico, T. E. Rogers, P. G. Ruminski, M. A. Russell, S. S. Yu, Int. Pat. Appl. WO1997036859A1; Chem. Abstr. 127 (1997) 346198.

[21] C. P. Briscoe, A. J. Peat, S. C. McKeown, D. F. Corbett, A. S. Goetz, T. R. Littleton, D. C. McCoy, T. P. Kenakin, J. L. Andrews, C. Ammala, J. A. Fornwald, D. M. Ignar, S. Jenkinson. Br. J. Pharmacol. 148 (2006) 619-628.

[22] A. Ichimura, A. Hirasawa, T. Hara, G. Tsujimoto. Prostaglandins Other Lipid Mediat. 89 (2009) 82-88.

[23] D. Eisenberg, E. Schwarz, M. Komarony, R. Wall. J. Mol. Biol. 179 (1984) 125-142.

[24] J. A. Ballesteros, H. Weinstein. Methods Neurosci. 25 (1995) 366-428.

[25] A. Srivastava, J. Yano, Y. Hirozane, G. Kefala, F. Gruswitz, G. Snell, W. Lane, A. Ivetac, K. Aertgeerts, J. Nguyen, A. Jennings. Nature 513 (2014) 124-127.

[26] Schrödinger Release 2017-2: Maestro, Schrödinger, LLC, New York, NY, 2017.

[27] Schrödinger Release 2017-2: Schrödinger Suite 2017-2 Protein Preparation Wizard; Epik, Schrödinger, LLC, New York, NY, 2016; Impact, Schrödinger, LLC, New York, NY, 2016; Prime, Schrödinger, LLC, New York, NY, 2017.

[28] I. G. Tikhonova, E. Poerio. BMC Struct. Biol. 15 (2015) 16.

[29] Schrödinger Release 2017-2: Jaguar, Schrödinger, LLC, New York, NY, 2017.

[30] E. Harder, W. Damm, J. Maple, C. Wu, M. Reboul, J. Y. Xiang, L. Wang, D. Lupyan, M. K. Dahlgren, J. L. Knight, J. W. Kaus. J. Chem. Theor. Comput. 12 (2015) 281-296.

[31] Schrödinger Release 2017-2: MacroModel, Schrödinger, LLC, New York, NY, 2017.

[32] Schrödinger Release 2017-2: LigPrep, Schrödinger, LLC, New York, NY, 2017.

[33] Schrödinger Release 2017-2: Glide, Schrödinger, LLC, New York, NY, 2017.

[34] The PyMOL Molecular Graphics System, Version 1.7, Schrödinger. LLC.

- Two 1,2,4-thiadiazole-based series of FFA1 agonists were designed and synthesized
- The two series stem from an earlier reported hit
- One of series with low micromolar potency is related to known FFA1 agonist GW9508
- The other, inactive series is a close analog of the earlier reported compounds
- Structural basis for the observed SAR findings is provided via docking simulation